

The influence of electronic and steric factors on chain branching in ethylene polymerization by Brookhart-type Ni(II) diimine catalysts: a combined density functional theory and molecular mechanics study

Tom K. Woo, Tom Ziegler *

Department of Chemistry, University of Calgary, 2500 University Drive, N.W., Calgary, Alberta, Canada T2N 1N4

Received 15 June 1999; accepted 23 July 1999

Abstract

Calculations have been carried out on the energy of ethylene complexation to the metal center in the Brookhart-type Ni(II) diimine olefin polymerization catalyst $(ArN=C(R)-C(R)=NAr)Ni(II)-CH_3^+$ for $C(R)-C(R)=CH-CH$; $C(Me)-C(Me)$ and $C-ANAP-C$ ($ANAP = acenaphthalene$). The goal of this study was to examine the influence of the $C(R)-C(R)$ substitution on the chain branching in the Brookhart Ni(II) diimine olefin polymerization catalysts. Experimental results suggest that the branching rates are controlled by the equilibrium between the π -complex and the metal alkyl. The branching rates were found experimentally to follow the trend $R=H < ANAP < CH_3$. It is shown that the trend in branching can be explained by the calculated order of olefin complexation $R=H > ANAP > CH_3$. It is further shown that the order of complexation energy is influenced by both electronic and steric factors. © 1999 Elsevier Science S.A. All rights reserved.

Keywords: Density functional theory; Molecular mechanism; Ethylene polymerization; Nickel

1. Introduction

Brookhart and coworkers [1–3] have recently developed Ni(II) and Pd(II) diimine-based catalysts of the type $(ArN=C(R)-C(R)=NAr)M-CH_3^+$, which have emerged as promising alternatives to both Ziegler–Natta and metallocene catalysts for olefin polymerization.

One of the most unique aspects of Brookhart's Ni diimine catalyst system is that a controlled level of short chain branching is possible with the homopolymerization of ethylene (Scheme 1). Normally, branching is introduced in polyethylene via the addition of short chain α -olefin comonomers, such as 1-hexene. Thus, this property is of commercial interest because it offers potential economic advantages. The degree of chain branching is observed to decrease with increasing monomer concentration, whereas both the activity and

molecular weights are found to be more or less independent of the monomer concentration [1–3]. Consistent with these observations, Johnson et al. [1,2] proposed the mechanism depicted in Fig. 1. Both the insertion and termination proceed from the π -complex which has been identified as the catalyst resting state. The branching, however, is believed to proceed from the naked metal alkyl complex via an isomerization mechanism. The monomer concentration effect on the chain branching can then be explained in terms of the equilibrium or kinetics involving the metal alkyl complex and the π -complex. The higher monomer concentrations, the faster the π -complex is formed and the less time there is to allow the isomerization process to take place from the metal alkyl complex. Therefore, the observed amount of branching diminishes with increased monomer concentration.

Increasing the steric bulk of the R substituents (Scheme 1) on the aryl rings dramatically increases the amount of branching that is observed. This can be explained in a straightforward manner with the pro-

* Corresponding author. Fax: +1-403-2899488.

E-mail address: ziegler@zinc.chem.ucalgary.ca (T. Ziegler)

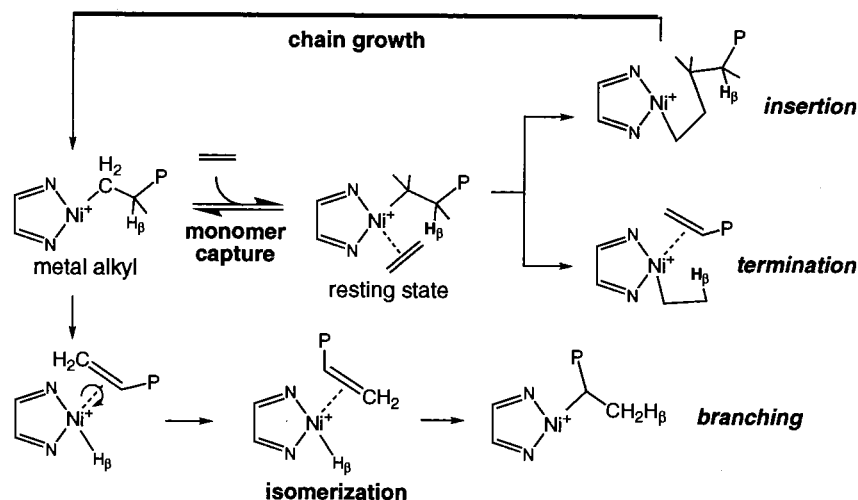
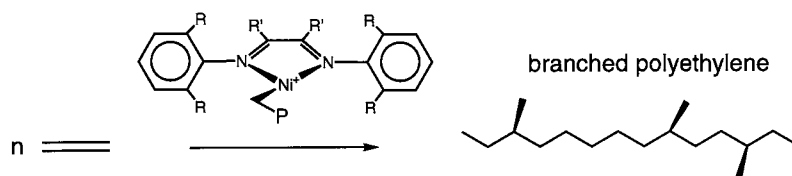


Fig. 1. Proposed chain branching mechanism in Brookhart's Ni(II) diimine olefin polymerization catalyst system. Unlike the insertion and termination, the chain branching is proposed to proceed from the metal alkyl complex.

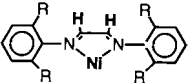
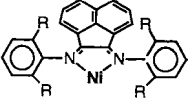
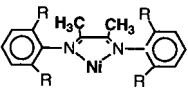
posed mechanism of Fig. 1 in terms of the capture process. Brookhart and Johnson [1,2] have argued that increasing the bulk of the aryl substituents has the effect of hindering access of the olefin to the metal center. This has the effect of shifting the equilibrium towards the free alkyl, thus allowing for more branching to occur. Our previous QM/MM and pure QM calculations [4,5] also agree with this argument since we find that the barrier of isomerization is not substantially influenced by the aryl substituents.

Another interesting chain branching substituent effect that has been observed experimentally involves the pendant R' group of the diimine ring. Table 1 details the observed experimental trends in terms of the amount of chain branching found in the resultant polymer versus the R substitution. In each case the substituent on the aryl group are the same ($R = i\text{-Pr}$), and the polymerization conditions are identical (in toluene with MAO cocatalyst at 0°C with ethylene at 1 atm pressure). With $R' = \text{H}$, the lowest amount of chain branching is observed with only 7.0 branches per 1000 carbons (C) of the polymer chain. Conversely, with $R' = \text{CH}_3$ in **3**, the chain branching occurs with the highest frequency at 48.0 branches per 1000 carbons. When the pendant R groups are replaced with an acenaphthalene (ANAP) substituent as in **2**, an interme-

diate amount of chain branching is observed with 24 branches per 1000 C. It is important to note that the amount of branching observed is dependent upon both the rate of branching and the rate of chain growth. For example, if we consider the rate of branching to be constant, then an increased rate of chain growth will result in less branching, and vice versa. By taking into account the rate of chain growth, which is shown in Table 1 in terms of the catalyst activity, the observed branches per 1000 C has been normalized to the activity observed with catalyst **3** in the last column. The normalized values provide an estimate of the rate (as opposed to the amount) of chain branching in each of the systems in relative terms. Table 1 reveals that the same overall trends are observed with the rates of chain branching as with the amount of chain branching. However, we notice that the disparity in branching between catalysts **2** and **3** is dramatically reduced upon considering the normalized data.

Since the R' substituents are physically removed from the active site, they cannot directly block the access of the olefin to the metal center as do the R substituents on the aryl rings. Thus, the effect has been assumed to be electronic in nature [6] Based on our previous combined QM/MM study [4,5] we suggest that there may be an indirect steric effect at work as well. The aryl rings, which prefer an orientation parallel to the central

Table 1
Experimental chain branching data

Catalyst structure (R = <i>i</i> -Pr)	Structure no.	Activity (kg mol ⁻¹ h ⁻¹)	Branches per 1000 C	
			Raw	Normalized to activity of catalyst 3
	1	6118	7.0	14
	2	5301	24.0	42
	3	3000	48.0	48

diimine ring due to an enhanced conjugation, are inhibited to do so by substitution in the R' position. The greater the hindrance, the more perpendicular the aryl rings become to the diimine ring. This has the effect of closing the active site as depicted in Fig. 2 for R' = H and CH₃. Fig. 2 reveals that with the smaller R' = H substituent, the aryl rings can assume a more parallel orientation, thus opening up one side of the metal center for olefin capture. Thus, the substitution in the R' position may have both an indirect steric influence in addition to the electronic influence on the capture equilibrium/barrier.

As previously noted, both theoretical [4–9] and experimental [1–3] results suggest that the equilibrium or possibly the kinetics between the metal alkyl and the π -complex control the rate of branching with the isomerization process playing a less consequential role. In all of the theoretical studies of Brookhart's catalyst that have recently appeared [4–9] none have examined the olefin capture process from naked alkyl to the π -complex in any details. In the present investigation we examine the interesting R' substitution effect on the chain branching rates as shown in Table 1. If the branching is controlled by the equilibrium between the naked alkyl and the π -complex, then the effect of the substitution can be determined by examining the thermochemistry of the naked alkyl versus the π -complex.

2. Computational details

For the model QM system (ArN=C(R)–C(R)=NAr)Ni–X⁺; Ar=R=H) all calculations were carried out by the Amsterdam Density Functional program pack-

age ADF [7]. The electronic configurations of the molecular systems were described by a triple- ζ basis set on nickel [8] for 3s, 3p, 3d, 4s, and 4p. Double- ζ STO basis sets were used for carbon (2s, 2p), hydrogen (1s) and nitrogen (2s, 2p), augmented with a single 3d polarization function except for hydrogen where a 2p function was used. The 1s²2s²2p⁶ configuration on nickel and the 1s² shell on carbon and nitrogen were assigned to the core and treated within the frozen core approximation. A set of auxiliary [8c] s, p, d, f, and g STO functions, centered on all nuclei, was used in order to fit the molecular density and present Coulomb and exchange potentials accurately in each SCF cycle. Energy differences were calculated by augmenting the local exchange-correlation potential by Vosko et al. [9] with Becke's [10] nonlocal exchange corrections and Perdew's [11] nonlocal correlation correction. Geometries were optimized including nonlocal corrections. First-order scalar relativistic corrections [12] were added to the total energy, since a perturbative relativistic approach is sufficient for 3d metals. In view of the fact that all systems investigated in this work show a large HOMO–LUMO gap, a spin restricted formalism was used for all calculations.

All stationary points for the real species 1, 2 and 3 of Table 1 have been optimized with the ADF-QM/MM program using a modified version [13] of the original IMOMM coupling scheme of Maseras and Morokuma [14]. Fig. 3 depicts the QM/MM partitioning of the full Ni-diimine catalyst, (ArN=C(R)–C(R)=NAr)Ni–X⁺ where R = CH₃ and Ar = Ar=2,6-C₆H₃(*i*-Pr)₂, 3. Carbon atoms in Fig. 3 labeled with asterisks represent the MM-link atoms at the QM/MM boundary. Use has been made of a link bond ratio [13], α , of 1.385 for the N–C(aryl) link bond in order to reproduce the average

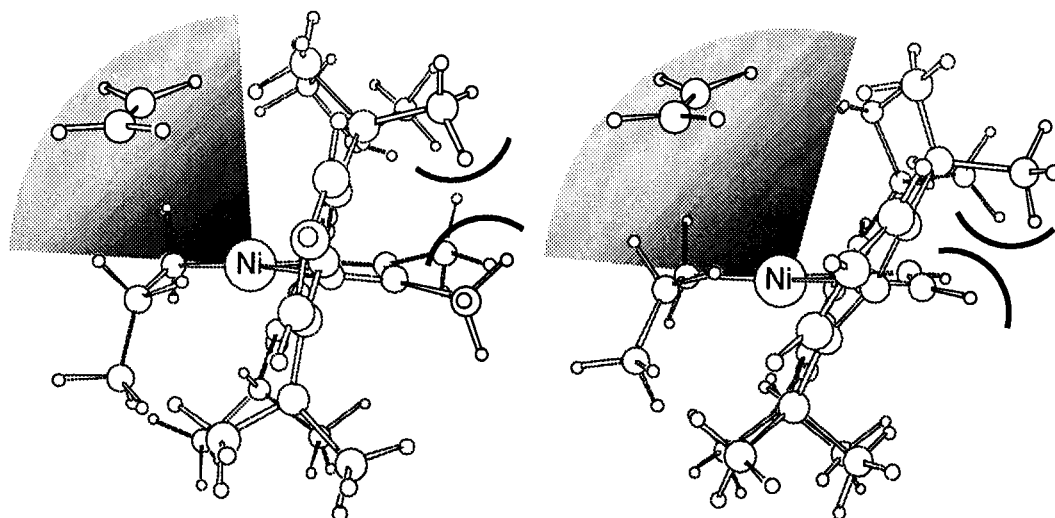


Fig. 2. The QM/MM partitioning of the Ni-diimine catalyst, $(\text{ArN}=\text{C}(\text{CH}_3)-\text{C}(\text{CH}_3)=\text{NAr})\text{Ni}-\text{R}^+$ used in this study. (a) The so-called real system where the link bonds are labeled with asterisks. (b) The QM model system.

bond distance of 1.44 Å observed in related experimental X-ray crystal structures [15]. In calculations where the pendant R' group is treated in the MM region, a link bond ratio of 1.38 was adopted when R' = CH₃ and a ratio of $\alpha = 1.34$ was used when R' = ANAP. In these cases, the link bond ratios were adjusted to reproduce the bond distances from calculations where the R' group is included in the QM region.

An augmented AMBER95 force field [16] was utilized to describe the molecular mechanics potential. Employing the AMBER atom type labels as described in Ref. [16], the diimine carbon was assigned with atom type CM parameters, the diimine N with N2, aryl ring carbon atoms with CA, aryl ring hydrogen atoms with HA and the remaining carbon and hydrogen atoms of the MM region with CT and HC, respectively. For the propagation and termination processes, the reacting ethene monomer was assigned with sp² C van der Waals parameters through to the transition state structure and changed to sp³ CT parameters in the product. A similar procedure was followed for the isomerization process. Alkyl carbon and hydrogen atoms of the active site were assigned CT and HC van der Waals parameters, respectively. Ni was assigned the Ni4 + 2 van der Waals parameters of Rappé's UFF [17]. Electrostatic interactions were not included in the molecular mechanics potential.

In this study, structural optimization of the QM/MM complexes involved a global minimum search of the MM subsystem [13b] with the QM subsystem frozen [13]. The global minimum search involved performing 100 ps of molecular dynamics on the MM subsystem at 800 K where structures were sampled every 2 ps. Each of the 50 sampled structures was then partially optimized. The best ten of these partially optimized structures was then fully optimized. The resulting lowest

energy structure was considered to be the global minimum for the particular frozen QM geometry. During the full optimization of the QM/MM system, the global minimum search was performed once at the beginning to provide the best initial MM structure for the given QM structure. The global search was not used in subsequent geometry optimization cycles. However, upon convergence of the geometry optimization, the global search was repeated in order to ensure that a new global MM minimum did not evolve as the QM subsystem changed. If the resulting structure was found to be more stable than the original by 0.2 kcal mol⁻¹, then the whole QM/MM optimization process was repeated starting from this new structure.

Ethene binding energies were calculated as the total energy of the olefin π -complex subtracted from the total energy of the free metal alkyl complex plus the free ethene. For all complexes, the growing chain was modeled by a propyl group. The propyl group has been previously shown [18] to be an appropriate model for the growing chain since it accounts for the β - and γ -agostic interactions with the metal center.

3. Results and discussion

In this study we attempt to correlate the olefin binding energy to the rate of chain branching that is observed experimentally, in order to elicit the nature of the branching control. We are making two primary assumptions here. First, we assume that the equilibrium between the free alkyl and the π -complex dominates the control of the branching rate. Thus, we are neglecting the influence of the capture barrier and the isomerization barrier on the branching rate. Since it is really the free energy difference ΔG° that is directly related to the

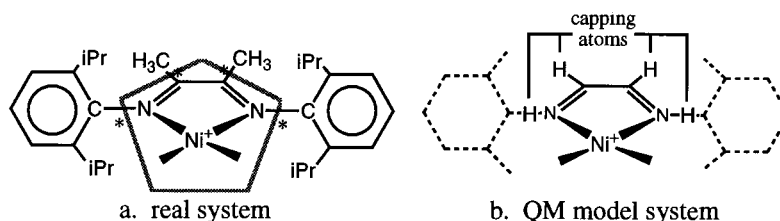


Fig. 3. Possible indirect steric effect of the R' diimine substituents on the monomer capture process.

Table 2
Capture energies without steric effects

Pure QM structures	Structure no.	$\Delta E_{\text{capture}}$ (kcal mol ⁻¹)
	1a	-16.9
	2a	-14.7
	3a	-15.0

equilibrium constant, the second assumption we are making is that the trends in olefin binding energy will be the same as the free energy trends. Since the binding energies are generally fairly substantial for cationic single-site catalysts [19a], this is a reasonable approximation according to standard enthalpy–entropy compensation arguments [19b–19d]. The goal in this study is not to quantify the equilibrium between the free alkyl and the π -complex, but rather to determine the nature of the R' substituent effect in (ArN=C(R')–C(R')=NAr)M–CH₂P⁺ on the branching.

3.1. Electronic factors

We first try to correlate the branching rates to the capture energy as a pure electronic effect of the R' substitution. For this purpose, the catalyst systems without the aryl rings (Ar=H) should be a good model, since in their absence the indirect steric interactions cannot occur. Therefore, if the R' substituents are treated at the QM level, the trends seen in the capture energy will be purely electronic in nature. We will assign these model systems for catalysts **1**, **2**, **3** the **a** sub-label to indicate that the aryl rings have been replaced with hydrogen atoms and that the systems are treated purely at the QM level. The olefin binding energies with model systems **1a**, **2a** and **3a** are given in Table 2.

Comparing the binding energies of **3a** and **1a** where R' = CH₃ and H, respectively, we note that the electronic effect of the CH₃ substitution is to reduce the binding energy. If we compare this result to the observed branching rates presented in Table 1, we note that the trend is compatible with our proposed model. In other words, since the binding energy is decreased upon replacement of R' = H with R' = CH₃, the equilibrium is shifted towards the metal alkyl complex in **3a** where more branching can occur. When the binding energy of **2a** with the ANAP substituent is considered, we find that it does not follow the observed trends in the branching rates. Whereas the rate of branching for catalyst **2** lies between those of **1** and **3**, the binding energy of **2a** is the smallest of all the systems.

Although the binding energies for **1–3a** do not correlate exactly with the branching data, we can explain the trends observed in Table 2 in terms of the π -donating abilities of the R' substituents. We first consider the nature of the interaction between the olefin and the metal center in the π -complex. As is commonly done, we separate the π -bonding into two components. The first component involves the donation of electron density from the π -orbital of the olefin to the empty d orbitals of the metal. Conversely, the second component involves the back-donation of charge density from the Ni center to the empty π^* orbitals of the metal.

Although the Ni has a formal d-electron count of eight, theoretical calculations show the presence of little back donation in the π -complexation [20]. Distortion of the bound ethene moiety can be used as a metric of this, since the more back-bonding there is present the longer the olefinic C–C bond becomes. Table 3 shows that the calculated olefin C–C bonds in all three π -complexes of **1–3a** are approximately 1.39 Å, an elongation of only 0.07 Å from the free ethene value which is calculated to be 1.32 Å. Such an elongation is typical of that observed in d⁰ metal olefin π -complexes were there is negligible back-donation because of the low d-electron count. Thus, the olefin binding in the Ni diimine systems appears to be dominated by the donation of olefin π -density into the empty d-orbitals of the metal center. Therefore, the more electron-deficient the Ni center is, the stronger the olefin binding becomes. Table 3 gives the net atomic charges on the Ni in the alkyl complex based on a Mulliken population analysis. The

Table 3
The effect of R' substitutions on the charge density on Ni and the back-bonding in the π -complex

Model	Ni charge in alkyl complex (e) ^a	Olefinic C–C distance in π -complex (Å)
1a	+0.546	1.389
2a	+0.487	1.394
3a	+0.505	1.391

^a Mulliken charge analysis.

results show that the order of electron deficiency, $R' = H > CH_3 > ANAP$, is consistent with the binding energies in Table 2. In terms of the R' groups, the better the π -donor ability of the substituent, the more electron density it is capable of donating to the metal and therefore the smaller the olefin binding energy. The trends in the binding energy expressed in Table 2 are consistent with this model since π -donor ability of the substituents is generally ordered as $H \ll Me \sim < \text{aryl}$ [21].

3.2. Steric factors

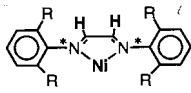
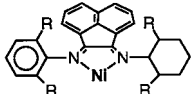
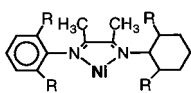
If the R' substituent effect is purely steric in nature, then a model system in which the electronic effects of the substituents are removed can be used to test the hypothesis. With the QM/MM method, we can construct just such a model where the various R' substituents are modeled by a MM potential, and the electronic effects are kept constant by using the same model QM system. In this way, catalysts **1–3** can be modeled such that the $(HN=CH-CR=NH)Ni-Pr^+$ molecule is used for the QM model system, while the aryl rings and the R' substituents are treated by the

AMBER95 force field. We will assign these purely steric model systems the **b** sub-label. Shown in Table 4 are the calculated olefin binding energies using the purely steric models **1b**, **2b** and **3b**. First we note that the QM component of the binding energies all reside close to 18 kcal mol⁻¹. This is to be expected since the QM models systems are the same in each calculation. The small variations in QM component of the capture energies are a result of the different steric environments presented by the catalyst framework due to the variation of the R' substituents.

The indirect steric effect as we have called it can be examined in more detail by comparing the olefin capture results of models **1b** and **3b**, where there is a 2.4 kcal mol⁻¹ shift in the capture energy upon modifying $R' = H$ to $R' = CH_3$. First, recall that there is an electronic preference for the aryl rings to be aligned parallel to the diimine rings as to maximize π -density overlap and conjugation of the rings. Conversely, the electronically least favorable orientation of the aryl rings is perpendicular to the diimine rings where there is a minimal amount of π -overlap. In our QM/MM potential, this effect is modeled by a molecular mechanics N(diimine)–C(aryl) torsional potential. The torsional energy is related to the torsional angle θ between the diimine ring plane and the aryl ring planes. When θ is 0 or 180° the diimine ring and the aryl ring are exactly parallel with one another, thus maximizing the conjugation. (Incidentally, in these systems such plane angles are physically unattainable because the *i*-Pr groups of the aryl rings would crash into the both the R' group and the Ni center.) Similarly, when θ is 90°, the two rings are perpendicular to one another and there is no stabilization due to the ring conjugation.

Fig. 4 shows the structures the metal alkyl complex and the olefin π -complex for both structures **1b** ($R' =$

Table 4
Capture energies without electronic influence of the R' substituents

QM/MM structures ^{a,b}	Model	$\Delta E_{\text{capture}}$ (kcal mol ⁻¹)	ΔE_{QM} (kcal mol ⁻¹)	ΔE_{MM} (kcal mol ⁻¹)
	1b	-16.1	-17.7	+1.63
	2b	-16.0	-18.5	+2.47
	3b	-13.7	-18.8	+5.12

^a Asterisks denote the QM/MM link bonds.

^b In all cases the QM model system is $(HN=CH-CR=NH)M-Pr^+$.

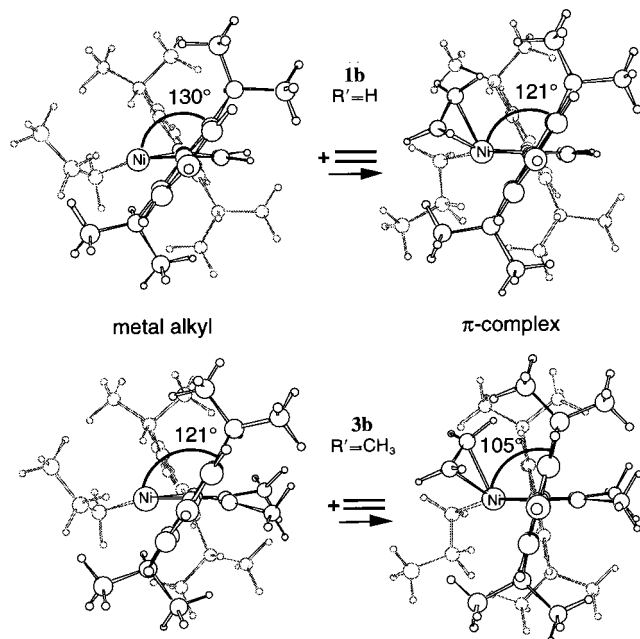


Fig. 4. Optimized metal alkyl and π -complex structures of the model systems **1b** and **3b**. The ring plane angle, θ , of the foremost aryl ring is shown for each structure. The backmost aryl ring and the alkyl chain are ghosted for clarity.

H) and **3b** ($R' = \text{CH}_3$). The structures are oriented such that the N(diimine)–C(aryl) bonds lie perpendicular to the plane of the page as to emphasize the plane angles between the aryl rings and the central Ni-diimine ring. Also shown are the ring plane angles of the foremost ring of each of the four structures. Without the complexed olefin, the propyl chain in the metal alkyl complexes lies roughly in the plane of the Ni-diimine ring. Since the alkyl coordination sites of the Ni center are vacant, this allows the aryl rings to align themselves in a more parallel fashion to the Ni-diimine ring. In doing so, an *i*-Pr group of one aryl ring partially occupies one axial site of the metal center while an *i*-Pr group from the other aryl ring fills up the opposite axial site. In **3b** the ring plane angle is 121° whereas it is slightly larger in **1b**. Here the larger methyl group of **3b** prevents the ring from swinging back as much compared to that in **1b**.

Upon formation of the π -complex, the propyl group shifts to occupy one axial site of the Ni center since the olefin coordinates to the opposite site. The formation of the π -complex therefore forces the aryl rings to assume a more perpendicular orientation as to accommodate the olefin and alkyl chain. For model **1b**, the olefin complexation causes the plane angle in the foremost ring (Fig. 4) to shrink by 9° from 130 to 121° . However, in model **3b** for which $R' = \text{CH}_3$, the effect is more severe with the plane angle shrinking by 16° from 121 to 105° upon olefin complexation. Thus, the complexation of the olefin more severely distorts the orientation

Table 5

Change in geometry and energy components during olefin complexation

Model	Change in plane angle ($\Delta\theta$)			
	<i>a</i> ($^\circ$) ^a	<i>b</i> ($^\circ$)	ΔE_{tors}	ΔE_{vdw}
1b	–8.7	–5.6	4.16	–2.17
2b	–9.4	–2.1 ^b	5.51	–2.92
3b	–16.0	–16.9	7.50	–0.21

^a Same as the foremost ring plane angle displayed in Fig. 3.

^b The ring plane angle here actually changes from 60.4 to 110.2° , but the deviation from the 90° , which has the energetic consequences, changes by -2.1° upon olefin complexation.

of the aryl rings away from their preferred orientation in **3b** compared to **1a**. In our QM/MM potential, this has the effect of increasing the MM torsion energy. Summarized in Table 5 are the changes in the plane angles and MM torsion energy upon coordination of the olefin. We notice that the larger change in plane angles incurred **3b** is reflected in a more unfavorable increase in the torsion energy. Specifically, the change in torsion energy, ΔE_{tors} , in **3b** is $7.5 \text{ kcal mol}^{-1}$ whereas it is only $4.16 \text{ kcal mol}^{-1}$ in **1b**. Also provided in Table 5 is the change in non-bonded van der Waals energy upon olefin complexation. The net values are negative because of the long range attractive component of the van der Waals potentials. (This effect has been previously observed with gas-phase combined QM/MM and pure MM calculations of coordination complexes [22].) The change in van der Waals energy upon complexation is $-2.17 \text{ kcal mol}^{-1}$ in **1b** whereas it is only $-0.21 \text{ kcal mol}^{-1}$ in **3b**. The more repulsive van der Waals complexation energy in **3b** can be explained in terms of the increased steric repulsion that occurs between the $R' = \text{CH}_3$ groups and the *i*-Pr groups which parallels the unfavorable perpendicular orientation of the aryl rings relative to the central Ni-diimine ring.

The steric demands of the $R' = \text{ANAP}$ substituent of **2b** can be expected to be somewhere between that of the $R' = \text{H}$ and $R' = \text{CH}_3$ substituents of **1b** and **3b**, respectively. Like the $R' = \text{H}$ substituent in **1b**, the atoms of the $R' = \text{aryl}$ substituent in **2b** lie in the plane of the Ni-diimine plane. However, the steric demands of the $R' = \text{ANAP}$ group can be expected to be slightly larger due to the fact that the van der Waals radius of C is about 30% larger than H and that the aryl group extends out further than the $R' = \text{H}$ does. Conversely the steric demands of the aryl group will be less than the methyl group, whose hydrogen atoms project out of the Ni-diimine plane, thus enhancing the interaction with the *i*-Pr groups. Table 4 shows that the olefin complexation energy with model **2b** is $16.0 \text{ kcal mol}^{-1}$, matching that of **1b**. Table 5 reveals that the change in

plane angle is roughly equivalent to that observed in **1b**. This suggests that the steric demands of the $R' = \text{aryl}$ substituent are similar to those of $R' = \text{H}$ in this context. The change in torsion energy upon complexation is $5.51 \text{ kcal mol}^{-1}$. This is $1.4 \text{ kcal mol}^{-1}$ higher than the $4.16 \text{ kcal mol}^{-1}$ change observed with **1b**. The higher ΔE_{tors} in **2b** compared to that of **1b** can be accounted for in the torsional distortions in the ANAP group due to the interaction with the *i*-Pr groups of the aryl rings. Although the steric demands of **2b** can be estimated to be slightly more than **1b**, the van der Waals energy of complexation is actually enhanced. This seemingly contradicts the correspondence between the two. However, we notice that the $R' = \text{ANAP}$ substituent has more atoms than either the $R' = \text{H}$ or $R' = \text{CH}_3$ groups, which corresponds to more van der Waals interactions between the R' groups and the olefin that all lie in the long-range attractive region of the potentials. Such a counter-intuitive size dependence with complexation energies has been previously observed with molecular mechanics studies of phosphine coordination energies with transition metals [22]. Here it was found that using a standard Lennard-Jones potential the phosphine coordination energies were actually found to be enhanced with increasing size and cone angle due to this effect. Thus, in this QM/MM model the olefin binding energy of **2b** relative to that of **1b** and **3b** is slightly over estimated.

The olefin binding energies of the purely steric model, **b**, do not correlate well with the observed branching rates presented in Table 1. Whereas the branching rate of the $R' = \text{ANAP}$ catalyst, **2**, lies close to the extreme of the $R' = \text{CH}_3$ catalyst, **3**, the purely steric model places the olefin binding energy of **2b** much closer to **1b** than **3b**. If we admit to a slight overbinding of the olefin due to the van der Waals potential in model **2b** then the correlation is improved to a small degree.

The purely electronic model, **a**, and the purely steric model, **b**, produced opposing trends in the olefin binding energy, neither of which correlated well with the branching rates. This suggests that the indirect steric effect may play a larger role than previously thought in controlling the olefin binding energy. We now incorporate both the electronic and steric effects of the R' substituents in our model QM/MM potential. In this new model, which we sub-label **c**, the R' groups are relegated to the QM region such that their electronic effects are included in the potential. However, unlike the pure electronic model, the indirect steric effect is accounted for in the present treatment by including the aryl rings in the MM region. The electronic effects of the R' substituents are included in this treatment since they are part of the QM subsystem whereas in the previous models, **b**, they were treated in the MM region. (With this being the only difference, the optimized structures of the catalyst framework from the two

models should be similar. Comparison of the ring plane angles of each of the structures with their counterparts in the other model show good agreement in the geometries of **2b** and **3b** with **2c** and **3c** [23]. The RMS difference in the plane angles is only 3.2° with a maximum deviation of 7.2° .)

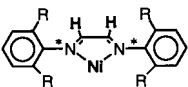
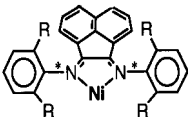
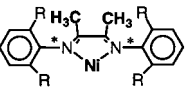
The capture energies for the mixed model, **c**, are given in Table 6 for the $R' = \text{H}$, ANAP and CH_3 substituents. The correlation between the estimated capture energies and the branching rates provided in Table 1 are better with the present model than either the purely steric or electronic models. Most significantly the expected trend is clearly reproduced with the order of the olefin capture energy being $\text{H} > \text{ANAP} > \text{CH}_3$. In the mixed model, the QM component, ΔE_{QM} , of the total olefin binding energy follows the trends of the pure electronic model (Table 2).

We note that the electronic characteristics of the ANAP substituent appear to dominate its influence on the olefin binding energy. This is evidenced by the fact that the difference in olefin binding energies between the ANAP catalyst and the $R' = \text{H}$ system is the same in the present model as with the pure electronic model, **a** (Table 2). The results are therefore consistent with the notion that the planar ANAP substituent is only slightly more sterically demanding than the $R' = \text{H}$ substituent. Trends in MM component of the complexation energy given in Table 6 show an anomalously low ΔE_{MM} for the ANAP catalyst. Again this can be attributed to the size dependent overbinding of the van der Waals potentials as previously discussed. The difference in ΔE_{MM} for the ANAP system in models **b** and **c** ($+2.47$ vs. $+0.76 \text{ kcal mol}^{-1}$) is due to the fact that the torsional distortion of the ANAP substituent upon olefin complexation is accounted for in the MM energy in model **b** but in the QM energy in model **c**.

Whereas the influence of the ANAP substituent appears to be electronic in nature (relative to $R' = \text{H}$), the influence of the $R' = \text{CH}_3$ substituent can be attributed to both electronic and steric factors. The difference in olefin binding energy in the purely electronic and purely steric models are 1.9 and $2.4 \text{ kcal mol}^{-1}$, respectively. The combined effect as in modeled in **3c** is nearly additive with difference in olefin binding energy of $3.2 \text{ kcal mol}^{-1}$.

The energetic consequence of the indirect steric effect is largely dependent upon the molecular mechanics N(diimine)–C(aryl) torsional potential used. The stronger the barrier the more enhanced the steric effect is likely to be. The success we have attained with our earlier study of the Brookhart catalyst [4,5], suggests that the standard AMBER95 potential used is a reasonable approximation to the true potential. However, we admit to some uncertainty in this potential. Despite this, the results show that the never before considered indirect steric influence is real. Thus, we conclude that the observed branching rates can be correlated to both

Table 6
Capture energies with both steric and electronic effects incorporated

QM/MM structures ^a	Model	$\Delta E_{\text{capture}}$ (kcal mol ⁻¹)	ΔE_{QM} (kcal mol ⁻¹)	ΔE_{MM} (kcal mol ⁻¹)
	1c ^b	-16.1	-17.7	+1.63
	2c	-14.0	-14.8	+0.76
	3c	-12.9	-16.9	+4.00

^a Asterisks denote the QM/MM link bonds.

^b Structure **1c** is the same as that of **1b**. The results are repeated for comparison.

the steric demands of the R' substituent in addition to the electronic nature of the substituent. Thus, increased branching can be achieved by enhancing the π -donating ability of the R' substituent or by increasing its steric bulk.

4. Conclusions

The goal of this study was to examine the nature of the R' substitution on the chain branching in the Brookhart Ni(II) diimine olefin polymerization catalysts. The branching rates were found to follow the trend R' = H < ANAP < CH₃. Experimental results suggest that the branching rates are controlled by the equilibrium between the π -complex and the metal alkyl [1]. Since the pendant R' groups are removed from the active site of the metal center, it has been assumed that the exhibited trends in the branching rates are an electronic effect of the R' groups. However, we have suggested there may also be an indirect steric effect at work due to an interaction of the R' groups with the aryl rings. This interaction forces the aryl rings to adopt an orientation which restricts access to the active site. Thus, the bulkier the R' groups the more sterically encumbered the active site becomes and the less favorable the olefin complexation. Therefore, the proposed net effect of the indirect steric interaction of the R' groups with the aryl rings is to shift the equilibrium towards the metal alkyl complex as to allow more branching to occur.

To test this hypothesis, three model systems were constructed: **a**, a pure electronic model where the indirect steric interactions were impossible; **b**, a purely

steric model where the electron influence of the R' substituents were removed; and **c**, a mixed model where both steric and electronic effects were included. Each of the three models were evaluated in terms of how well the olefin binding energies correlated to the experimentally observed branching rates. The resulting olefin binding energies of neither the purely electronic model or the purely steric model reproduced the trends in the branching rates. With the purely electronic model, the binding energies were found to follow the trend R' = H > CH₃ > ANAP, whereas with the purely steric model the trend was R' = H \approx ANAP > CH₃. Both trends could easily be accounted for in terms of the electronic and steric characteristics of the R' substituents.

In the last model, where both the steric and electronic effects of the R' substituents were incorporated, the olefin binding energies were found to correlate well with the observed branching rates. Although the experimental data set is small, the results do suggest that both the steric and electronic characteristics of the R' substituents must be considered when tuning the chain branching capabilities of the catalyst. Recently, a number of promising olefin polymerization catalyst systems have appeared [24] that strongly resemble the basic structure of the Brookhart catalyst, in that they possess two aryl rings that act to block the axial coordination sites of the metal center. In some of these related systems, the central ring involving the metal center is not fully conjugated. Therefore, the electronic effects of the equivalent R' substituents in these systems may be significantly weaker than in the present catalyst system. Thus, the indirect steric effect may be more dominant in controlling the chemistry of the system. Indeed we

have utilized idea of the indirect steric effect to enhance the molecular weight properties of the Zr-McConville [25] catalyst.

It is very common in catalytic systems that there is a strong interplay between electronic and steric effects. We have demonstrated how the QM/MM methodology can be used to isolate and decompose the effects of each. In this capacity the QM/MM method has great potential to be used as an analytical tool to provide a deeper understanding of the catalytic control.

Acknowledgements

This investigation was supported by NSERC of Canada, as well as by the donors of the Petroleum Research Fund, administered by the American Chemical Society (ACS-PRF No. 31205-AC3).

References

- [1] L.K. Johnson, C.M. Killian, M. Brookhart, *J. Am. Chem. Soc.* 117 (1995) 6414.
- [2] L.K. Johnson, S. Mecking, M. Brookhart, *J. Am. Chem. Soc.* 118 (1996) 267.
- [3] S.A. Svejda, M. Brookhart, *Organometallics* 18 (1999) 65.
- [4] L. Deng, T.K. Woo, L. Cavallo, P.M. Margl, T. Ziegler, *J. Am. Chem. Soc.* 119 (1997) 6177.
- [5] L. Deng, P.M. Margl, T. Ziegler, *J. Am. Chem. Soc.* 119 (1997) 1094.
- [6] M. Brookhart, Department of Chemistry, University of North Carolina at Chapel Hill, personal communication.
- [7] (a) E.J. Baerends, D.E. Ellis, P. Ros, *Chem. Phys.* 2 (1973) 41. (b) E.J. Baerends, P. Ros, *Chem. Phys.* 2 (1973) 52. (c) E.J. Baerends, Ph.D. Thesis, Free University, Amsterdam, The Netherlands, 1975. (d) G. te Velde, E.J. Baerends, *J. Comput. Chem.* 99 (1992) 84.
- [8] (a) J.G. Snijders, E.J. Baerends, P. Vernoijs, *Atom. Nucl. Data Tables* 26 (1982) 483. (b) P. Vernoijs, J.G. Snijders, E.J. Baerends, Slater Type Basis Functions for the Whole Periodic System, Department of Theoretical Chemistry, Free University, Amsterdam, The Netherlands, 1981. (c) J. Krijn, E.J. Baerends, Fit Functions in the HFS Method, Department of Theoretical Chemistry, Free University, Amsterdam, The Netherlands, 1984.
- [9] S.H. Vosko, L. Wilk, M. Nusair, *Can. J. Phys.* 58 (1980) 1200.
- [10] A. Becke, *Phys. Rev. A* 38 (1988) 3098.
- [11] (a) J.P. Perdew, *Phys. Rev. B* 34 (1986) 7406. (b) J.P. Perdew, *J. Phys. Rev. B* 33 (1986) 8822.
- [12] (a) J.G. Snijders, E.J. Baerends, *Mol. Phys.* 36 (1978) 1789. (b) J.G. Snijders, E.J. Baerends, P. Ros, *Mol. Phys.* 38 (1979) 1909.
- [13] (a) T.K. Woo, L. Cavallo, T. Ziegler, *Theor. Chem. Acta* 100 (1998) 307. (b) T.K. Woo, PhD Thesis, University of Calgary, Canada, 1998.
- [14] F. Maseras, K. Morokuma, *J. Comput. Chem.* 16 (1995) 1170.
- [15] (a) J.C.M. Sinnema, G.H.B. Frensdak, H. tom-Dieck, *J. Organomet. Chem.* 390 (1990) 237. (b) R. Diercks, J. Kopf, H. tom-Dieck, *Acta Crystallogr. Sect. C* 40 (1984) 363. (c) R. van-Asselt, C.J. Elsevier, W.J.J. Smeets, A.L. Spek, *Inorg. Chem.* 33(1994) 1521.
- [16] W.D. Cornell, P. Cieplak, C.I. Bayly, I.R. Gould, K.M. Merz Jr., D.M. Ferguson, D.C. Spellmeyer, T. Fox, J.W. Caldwell, P.A. Kollman, *J. Am. Chem. Soc.* 117 (1995) 5179.
- [17] A.K. Rappé, C.J. Casewit, K.S. Colwell, W.A. Goddard III, W.M. Skiff, *J. Am. Chem. Soc.* 114 (1992) 10024.
- [18] T.K. Woo, P. Margl, J.C.W. Lohrenz, P.E. Blöchl, T. Ziegler, *J. Am. Chem. Soc.* 118 (1996) 13021.
- [19] (a) P.M. Margl, L. Deng, T. Ziegler, *Organometallics* 17 (1998) 933. (b) M.S. Searle, D.H. Williams, *J. Am. Chem. Soc.* 114 (1992) 10690. (c) J.D. Dunitz, *Chem. Biol.* 2 (1995) 709. (d) J.D. Dunitz, *Science* 264 (1994) 670.
- [20] L. Deng, P.M. Margl, T. Ziegler, *J. Am. Chem. Soc.* 119 (1997) 1094.
- [21] A. Rauk, *Orbital Interaction Theory of Organic Chemistry*, Wiley, New York, 1994.
- [22] (a) T.K. Woo, T. Ziegler, *Inorg. Chem.* 33 (1994) 1857. (b) L. Cavallo, T.K. Woo, T. Ziegler, *Can. J. Chem.* 76 (1998) 1457.
- [23] Models **1b** and **1c** are the same.
- [24] (a) J.D. Scollard, D.H. McConville, *J. Am. Chem. Soc.* 118 (1996) 10008. (b) B.L. Small, M. Brookhart, A.M.A. Benett, *J. Am. Chem. Soc.* 120 (1998) 4049. (c) J.D. Scollard, D.H. McConville, N.C. Payne, J. Vittal, *Macromolecules* 29 (1996) 5241. (d) G.J.P. Britovsek, V.C. Gibson, B.S. Kimberley, P.J. Maddox, S.J. McTavish, G.A. Solan, A.J.P. White, D.J. Williams, *Chem. Commun.* (1998) 849. (e) R. Baumann, W.M. Davis, R.R. Schrock, *J. Am. Chem. Soc.* 119 (1997) 3830.
- [25] L. Deng, T. Ziegler, T.K. Woo, P.M. Margl, L. Fan, *Organometallics* 17 (1998) 3240.